



Contents lists available at ScienceDirect

Food Chemistry

journal homepage: [www.elsevier.com/locate/foodchem](http://www.elsevier.com/locate/foodchem)

## Novel inhibitors of tyrosinase produced by the 4-substitution of TCT

Jian Xu<sup>a</sup>, Jing Liu<sup>a</sup>, Xinqi Zhu<sup>a</sup>, Yanying Yu<sup>a</sup>, Shuwen Cao<sup>a,b,\*</sup>

<sup>a</sup> Department of Chemistry, Nanchang University, Nanchang 330031, PR China

<sup>b</sup> State Key Laboratory of Food Science and Technology, Nanchang University, Nanchang 330047, PR China

### ARTICLE INFO

#### Article history:

Received 26 February 2016

Received in revised form 10 October 2016

Accepted 28 October 2016

Available online xxxxx

#### Keywords:

Thiophene-2-carbaldehyde  
thiosemicarbazone (TCT) derivatives  
Tyrosinase inhibitors  
Fluorescence spectrum  
1H and 13C NMR titration

### ABSTRACT

We synthesized a series of 4- or 5-functionalized TCT derivatives (**1–12**) and investigated their inhibitory activities and mechanisms on tyrosinase by using Spectrofluorimetry, <sup>1</sup>H and <sup>13</sup>C NMR titration and IR spectra. The results of the fluorescence spectra and NMR titrations showed that the thiosemicarbazone moiety formed complexes with copper ions in the active center of the enzyme and played an important role in inhibiting the activities of the target compounds. The 5-functionalization decreased the inhibitory activity, but the 4-functionalization with a methoxyacetyl group enhanced the inhibitory activity, in which a strong auxiliary vicinity synergistic effect from the methoxyacetyl group strengthens and promotes the formation of complexes between the sulfur atoms of the inhibitor and the dicopper nucleus of tyrosinase. We concluded that the appropriate 4-functionalization improved the inhibitory activity of the modifier, and that 4-methoxyacetyl -TCT is promising for the inhibition of tyrosinase.

© 2016 Elsevier Ltd. All rights reserved.

### 1. Introduction

Tyrosinase (EC 1.14.18.1), a kind of metalloenzyme with dinuclear copper ions, is common in animals, insects and microorganisms (Song et al., 2006). Structurally, tyrosinase belongs to the Type-3 copper protein family, with two copper ions bonded in a coordinate and a distinct set of three histidine residues within the active site (Motabo, Kumagai, Yamamoto, Yoshitsu, & Sugiyama, 2006). Generally, tyrosinase is known as the rate-limiting enzyme involved in two-step oxidation for the transformation of L-tyrosine into dopaquinone, which is crucial for melanin biosynthesis (Seo, Sharma, & Sharma, 2003). Excessively active tyrosinase, which results in an over-accumulation of melanin in the human body, can cause a series of common skin diseases from freckles to malignant melanoma (Choi, Park, & Jee, 2015). Abnormal tyrosinase activity is related to Parkinson's disease (Pan, Li, & Jankovic, 2011). In addition, tyrosinase promotes cuticle formation in insects, which causes the browning of fruits and vegetables (Yin et al., 2015), and their subsequent loss of quality (Shi, Chen, Wang, Song, & Qiu, 2005). Preventing this unfavorable browning reaction is still a challenge in food science (Arung et al., 2005; Chen, Xing, Wang, Zheng, & Wang, 2015). Therefore, tyrosinase inhibitors with excellent inhibitory activities and lower side effects have promising applications in the fields of medicine, agriculture, food sciences and cosmetics.

Before this study, hundreds of tyrosinase inhibitors with good inhibition activities have been separated from nature or synthesized in laboratories (Chang, 2009; Mendes, Perry, & Francisco, 2014; Sabudak, Demirkiron, Ozturk, & Topcu, 2013), but only a few were studied for their structure-activity relationships, inhibitory mechanisms and structural modifications. Focusing on these particular properties of tyrosinase inhibitors could lead to the development of new and better inhibitors, although very few would be practical because of their toxicity, side effects, and low stability and solubility. In our prior study of a novel tyrosinase inhibitor, thiophene-2-carbaldehyde thiosemicarbazone (TCT), we obtained a preliminary understanding of the structure-activity relationships and inhibitory mechanisms between precursors and target enzymes by using fluorescence, <sup>1</sup>H NMR titration and molecular docking studies (Xie, Dong, Yu, & Cao, 2016). However, we still have little understanding of how the structure-activity relationships and inhibitory mechanisms affect the inhibitory activities when modifying TCT using the 4- and 5-functionalization of a thiophene ring on TCT. Generally, these types of structural modifications either increase or decrease the inhibitory activity of the modifier. Based on our understanding of the structure-activity relationship of TCT, we find it possible to increase the inhibitory activity of a modifier by introducing an appropriate functional group at the thiophene ring on TCT, assuming that the introduced group promotes the formation of complexes between the sulfur atom from the thiourea of target modifiers and the copper ion of the enzyme center. It is necessary to find new tyrosinase inhibitors

\* Corresponding author at: Department of Chemistry, Nanchang University, Nanchang 330031, PR China.

E-mail address: [caosw@ncu.edu.cn](mailto:caosw@ncu.edu.cn) (S. Cao).

with strong inhibitory activities to better our understanding of the structure-activity relationship of TCT.

In general excellent safety of precursor is the base and key to get a promising tyrosinase inhibitor used as food additive after structure modification. In order to evaluate and determine the safety of TCT as precursor of promising tyrosinase inhibitor, we obtained the toxicity data of TCT from <https://chem.sis.nlm.nih.gov>. The toxicity for mice (oral) is LD<sub>50</sub> 226 mg/kg (Guo et al., 1989), and for rats (oral) is LD 500 mg/kg. Further, a toxicity test of TCT was conducted before we began this study according to guiding principles of the drug acute toxicity test (CDER & FDA, 1996; Cordier, 1991). This test showed that the LD<sub>50</sub> of TCT was 808.83 mg/kg bw (orally given to female mice) and 912.48 mg/kg bw (orally given to male mice), which was of low toxicity and comparable to that commonly used in food additives in accord with F. D.A. guidelines of TBHQ (Tert-Butylhydroquinone, synthetic food additive, LD<sub>50</sub> 700–1000 mg/kg bw, orally given to rat), BHA (Butyl Hydroxy Anisol, synthetic food additive, LD<sub>50</sub> 1100 mg/kg bw, orally given to male mouse; 1300 mg/kg bw, orally given to female mouse). Therefore, from the toxicity and safety point of view, TCT was a good precursor for finding candidates for potential tyrosinase inhibitors of food additives.

A series of 4-functionalized and 5-functionalized TCT derivatives were designed, synthesized and evaluated for their inhibitory effects on tyrosinase. Spectrofluorimetry, <sup>1</sup>H and <sup>13</sup>C NMR titration, and IR spectra were used to investigate the interactions between these modifiers and tyrosinase. Our study helped clarify the relationship between modifiers and tyrosinase and provides a promising route to obtain novel tyrosinase inhibitors and highly potent tyrosinase inhibitors.

## 2. Materials and methods

### 2.1. Materials

Mushroom tyrosinase (EC 1.14.18.1) and L-3,4-dihydroxy phenyl-alanine (L-DOPA) were purchased from Sigma (St. Louis, MO, USA). 2-thiophenecarboxaldehyde and 5-Methyl-2-thiophene

carboxaldehyde were obtained from J&K Chemical Co (Shanghai, China). 5-Nitro-2-thiophenecarboxaldehyde and 5-Phenylthiophene-2-carbaldehyde were obtained from Zhengzhou Xipaike Chemical Co (Henan, China) and Accela ChemBio Co (Shanghai, China), respectively. All other reagents were local and of analytical grade. The water used was re-distilled and ion-free.

### 2.2. Synthesis

The method of synthesis of target compounds is described in Fig. 1, as reference (Zhu et al., 2009) described. The products are purified by recrystallization from ethanol and identified by ESI-MS, <sup>1</sup>H NMR and <sup>13</sup>C NMR analyses. ESI-MS data were obtained on a Bruker ESQUIRE-LC (Germany), <sup>1</sup>H NMR and <sup>13</sup>C NMR data were acquired on a 400 MHz NMR spectrometer (DD2-400) from Agilent (USA). The IR spectra were measured with KBr pellets on a Nicolet 5700 FT-IR spectrometer.

4-Hydroxymethyl-thiophene-2-carbaldehyde thiosemicarbazone (1): yellow solid, yield 85.2%, IR(KBr) 3421, 3151, 1601, 1532 cm<sup>-1</sup>; <sup>1</sup>H NMR (400 MHz, DMSO-*d*<sub>6</sub>) δ 11.37 (s, 1H, NH), 8.17 (s, 2H, NH<sub>2</sub>), 7.50 (s, 1H, CH), 7.36 (s, 1H, thiophene-H), 7.33 (s, 1H, thiophene-H), 5.13 (s, H, OH), 4.40 (s, 2H, CH<sub>2</sub>). <sup>13</sup>C NMR (400 MHz, DMSO-*d*<sub>6</sub>) δ 177.85(1C, C=S), 144.97(1C, C=N), 138.95 (1C, thiophene-C), 138.08(1C, thiophene-C), 130.59(1C, thiophene-C), 124.25(1C, thiophene-C), 59.14(1C, CH<sub>2</sub>). MS (ESI): *m/z* 214.0 [M-H].

4-Methoxymethyl-thiophene-2-carbaldehyde thiosemicarbazone (2): greyish yellow crystals, yield 76.4%, IR(KBr) 3160, 1609, 1525 cm<sup>-1</sup>; <sup>1</sup>H NMR (400 MHz, DMSO-*d*<sub>6</sub>) δ 11.40 (s, 1H, NH), 8.17 (s, 2H, NH<sub>2</sub>), 7.54 (s, 1H, CH), 7.47 (s, 1H, thiophene-H), 7.36 (s, 1H, thiophene-H), 4.32(s, 2H, CH<sub>2</sub>), 3.24 (s, 3H, CH<sub>3</sub>). <sup>13</sup>C NMR (400 MHz, DMSO-*d*<sub>6</sub>) δ 177.90(1C, C=S), 140.40(1C, C=N), 139.25(1C, thiophene-C), 137.86(1C, thiophene-C), 130.94(1C, thiophene-C), 126.35(1C, thiophene-C), 69.21(1C, CH<sub>2</sub>), 57.84(1C, CH<sub>3</sub>). MS (ESI): *m/z* 228.1 [M-H].

4-Ethoxymethyl-thiophene-2-carbaldehyde thiosemicarbazone (3): yellow solid, yield 74.3%, IR(KBr) 3149, 1597, 1522 cm<sup>-1</sup>; <sup>1</sup>H NMR (400 MHz, DMSO-*d*<sub>6</sub>) δ 11.39 (s, 1H, NH), 8.17 (s, 2H, NH<sub>2</sub>),

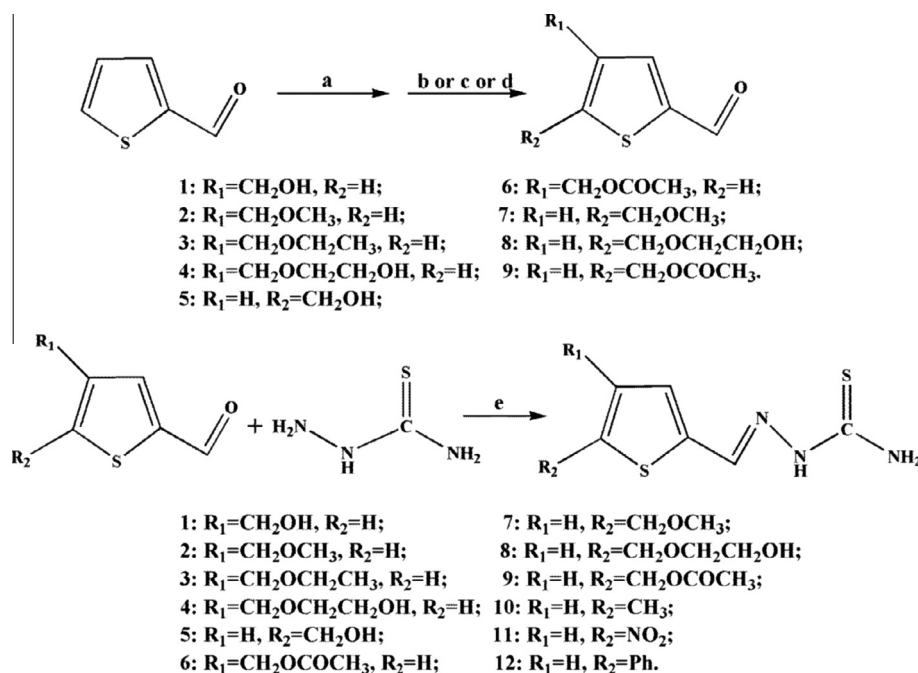


Fig. 1. Synthesis of 4-functionalized and 5-functionalized thiophene-2-carbaldehyde thiosemicarbazone derivatives 1–12; synthesis method (a): chloromethylation reaction; (b) etherification reaction; (c) esterification reaction; (d) hydrolysis reaction; and (e): methanol, acetic acid, reflux 2 h.

7.53 (s, 1H, CH), 7.45 (s, 1H, thiophene-H), 7.35 (s, 1H, thiophene-H), 4.35 (s, H, OH), 3.43 (m, 2H, CH<sub>2</sub>), 1.1(t, 3H, CH<sub>3</sub>). <sup>13</sup>C NMR (400 MHz, DMSO-*d*<sub>6</sub>) δ 177.89(1C, C=S), 140.79(1C, C=N), 139.21(1C, thiophene-C), 137.89(1C, thiophene-C), 130.97(1C, thiophene-C), 126.13(1C, thiophene-C), 67.28(1C, CH<sub>2</sub>), 65.34(1C, CH<sub>2</sub>), 57.84(1C, CH<sub>3</sub>). MS (ESI): *m/z* 242.1 [M-H]<sup>-</sup>.

4-(2-Hydroxy-ethoxymethyl)-thiophene-2-carbaldehyde thiosemicarbazone (**4**): pale yellow crystals, yield 84.1%, IR(KBr) 3441, 3178, 1608, 1528 cm<sup>-1</sup>; <sup>1</sup>H NMR (400 MHz, DMSO-*d*<sub>6</sub>) δ 11.39 (s, 1H, NH), 8.17 (s, 2H, NH<sub>2</sub>), 7.52 (s, 1H, CH), 7.47 (s, 1H, thiophene-H), 7.37 (s, 1H, thiophene-H), 4.60 (s, H, OH), 4.40 (s, 2H, CH<sub>2</sub>), 3.48(t, 2H, CH<sub>2</sub>), 3.42(t, 2H, CH<sub>2</sub>). <sup>13</sup>C NMR (400 MHz, DMSO-*d*<sub>6</sub>) δ 177.88(1C, C=S), 140.76(1C, C=N), 139.17(1C, thiophene-C), 137.90(1C, thiophene-C), 131.07(1C, thiophene-C), 126.18(1C, thiophene-C), 72.03(1C, CH<sub>2</sub>), 67.71(1C, CH<sub>2</sub>), 60.62(1C, CH<sub>2</sub>). MS (ESI): *m/z* 258.1 [M-H]<sup>-</sup>.

5-Hydroxymethyl-thiophene-2-carbaldehyde thiosemicarbazone (**5**): pale yellow acicular crystal, yield 74.9%, IR(KBr) 3439, 3166, 1589, 1549 cm<sup>-1</sup>; <sup>1</sup>H NMR (400 MHz, DMSO-*d*<sub>6</sub>) δ 11.36 (s, 1H, NH), 8.13 (d, 2H, NH<sub>2</sub>), 7.46 (s, 1H, CH), 7.25 (d, 1H, thiophene-H), 6.90 (d, 1H, thiophene-H), 5.53 (s, H, OH), 4.59 (s, 2H, CH<sub>2</sub>). <sup>13</sup>C NMR (400 MHz, DMSO-*d*<sub>6</sub>) δ 177.77(1C, C=S), 150.21(1C, C=N), 138.25(1C, thiophene-C), 137.62(1C, thiophene-C), 130.89(1C, thiophene-C), 124.74(1C, thiophene-C), 58.98(1C, CH<sub>2</sub>). MS (ESI): *m/z* 214.2 [M-H]<sup>-</sup>.

4-Methoxyacetyl-thiophene-2-carbaldehyde thiosemicarbazone (**6**): pale yellow flaky crystals, yield 73.1%, IR(KBr) 3155, 1742, 1601, 1531 cm<sup>-1</sup>; <sup>1</sup>H NMR (400 MHz, DMSO-*d*<sub>6</sub>) δ 11.40 (s, 1H, NH), 8.16 (s, 2H, NH<sub>2</sub>), 7.57 (s, 1H, thiophene-H), 7.53 (s, 1H, CH), 7.38 (s, 1H, thiophene-H), 4.40 (s, 2H, CH<sub>2</sub>), 2.03(s, 3H, CH<sub>3</sub>). <sup>13</sup>C NMR (400 MHz, DMSO-*d*<sub>6</sub>) δ 177.99(1C, C=S), 170.64(1C, C=O), 139.57(1C, C=N), 137.98(1C, thiophene-C), 137.69(1C, thiophene-C), 131.04(1C, thiophene-C), 127.64(1C, thiophene-C), 61.04(1C, CH<sub>2</sub>), 21.13(1C, CH<sub>3</sub>). MS (ESI): *m/z* 256.0 [M-H]<sup>-</sup>.

5-Methoxymethyl-thiophene-2-carbaldehyde thiosemicarbazone (**7**): yellow powder, yield 80.3%, IR(KBr) 3144, 1601, 1522 cm<sup>-1</sup>; <sup>1</sup>H NMR (400 MHz, DMSO-*d*<sub>6</sub>) δ 11.39 (s, 1H, NH), 8.15 (s, 2H, NH<sub>2</sub>), 7.50 (s, 1H, CH), 7.27 (d, 1H, thiophene-H), 6.98 (d, 1H, thiophene-H), 4.53 (s, 2H, CH<sub>2</sub>), 3.25(s, 3H, CH<sub>3</sub>). <sup>13</sup>C NMR (400 MHz, DMSO-*d*<sub>6</sub>) δ 177.87(1C, C=S), 144.44(1C, C=N), 139.00(1C, thiophene-C), 137.93(1C, thiophene-C), 130.67(1C, thiophene-C), 127.23(1C, thiophene-C), 68.82(1C, CH<sub>2</sub>), 57.78(1C, CH<sub>3</sub>). MS (ESI): *m/z* 228.0 [M-H]<sup>-</sup>.

5-(2-Hydroxy-ethoxymethyl)-thiophene-2-carbaldehyde thiosemicarbazone (**8**): pale yellow powder, yield 72.2%, IR(KBr) 3162, 1628, 1545 cm<sup>-1</sup>; <sup>1</sup>H NMR (400 MHz, DMSO-*d*<sub>6</sub>) δ 11.39 (s, 1H, NH), 8.16 (s, 2H, NH<sub>2</sub>), 7.50(s, 1H, CH), 7.27 (d, 1H, thiophene-H), 6.99 (d, 1H, thiophene-H), 4.62 (s, 2H, CH<sub>2</sub>), 3.49(t, 2H, CH<sub>2</sub>), 3.45(t, 2H, CH<sub>2</sub>). <sup>13</sup>C NMR (400 MHz, DMSO-*d*<sub>6</sub>) δ 177.72(1C, C=S), 145.04(1C, C=N), 138.90(1C, thiophene-C), 137.99(1C, thiophene-C), 130.68(1C, thiophene-C), 127.10(1C, thiophene-C), 71.91(1C, CH<sub>2</sub>), 67.42(1C, CH<sub>2</sub>), 60.58(1C, CH<sub>2</sub>). MS (ESI): *m/z* 258.1 [M-H]<sup>-</sup>.

5-Methoxyacetyl-thiophene-2-carbaldehyde thiosemicarbazone (**9**): pale yellow crystal, yield 81.1%, IR(KBr) 3174, 1723, 1611, 1536 cm<sup>-1</sup>; <sup>1</sup>H NMR (400 MHz, DMSO-*d*<sub>6</sub>) δ 11.43 (s, 1H, NH), 8.16 (s, 2H, NH<sub>2</sub>), 7.54(s, 1H, CH), 7.29 (d, 1H, thiophene-H), 7.10 (d, 1H, thiophene-H), 5.20 (s, 2H, CH<sub>2</sub>), 2.03(s, 3H, CH<sub>3</sub>). <sup>13</sup>C NMR (400 MHz, DMSO-*d*<sub>6</sub>) δ 177.95(1C, C=S), 170.13(1C, C=O), 141.07(1C, C=N), 140.11(1C, thiophene-C), 137.74(1C, thiophene-C), 130.57(1C, thiophene-C), 129.25(1C, thiophene-C), 60.59(1C, CH<sub>2</sub>), 21.06(1C, CH<sub>3</sub>). MS (ESI): *m/z* 258.0 [M + H]<sup>+</sup>.

5-Methyl-thiophene-2-carbaldehyde thiosemicarbazone (**10**): yellow powder, yield 86.6%, IR(KBr) 3148, 1590, 1524 cm<sup>-1</sup>; <sup>1</sup>H NMR (400 MHz, DMSO-*d*<sub>6</sub>) δ 11.37 (s, 1H, NH), 8.14 (s, 2H, NH<sub>2</sub>), 7.44(s, 1H, CH), 7.23 (d, 1H, thiophene-H), 6.81 (d, 1H, thiophene-

H), 2.50 (s, 3H, CH<sub>3</sub>). <sup>13</sup>C NMR (400 MHz, DMSO-*d*<sub>6</sub>) δ 177.70(1C, C=S), 143.22(1C, C=N), 138.24(1C, thiophene-C), 136.81(1C, thiophene-C), 131.48(1C, thiophene-C), 126.84(1C, thiophene-C), 15.80(1C, CH<sub>3</sub>). MS (ESI): *m/z* 200.0 [M + H]<sup>+</sup>.

5-Nitro-thiophene-2-carbaldehyde thiosemicarbazone (**11**): yellow powder, yield 84.2%, IR(KBr) 3470, 1608, 1540, 1335 cm<sup>-1</sup>; <sup>1</sup>H NMR (400 MHz, DMSO-*d*<sub>6</sub>) δ 11.77 (s, 1H, NH), 8.41, 8.17 (d, 2H, NH<sub>2</sub>), 8.06 (d, 1H, thiophene-H), 8.00(s, 1H, CH), 7.51 (d, 1H, thiophene-H). <sup>13</sup>C NMR (400 MHz, DMSO-*d*<sub>6</sub>) δ 178.55(1C, C=S), 151.50(1C, C=N), 147.19(1C, thiophene-C), 135.67(1C, thiophene-C), 130.88(1C, thiophene-C), 129.66(1C, thiophene-C). MS (ESI): *m/z* 229.1 [M-H]<sup>-</sup>.

5-Phenyl-thiophene-2-carbaldehyde thiosemicarbazone (**12**): yellow powder, yield 83.7%, IR(KBr) 3164, 1589, 1521 cm<sup>-1</sup>; <sup>1</sup>H NMR (400 MHz, DMSO-*d*<sub>6</sub>) δ 11.47 (s, 1H, NH), 8.19 (s, 2H, NH<sub>2</sub>), 7.67 (d, 2H, Ph-H), 7.55(s, 1H, CH), 7.49 (d, 1H, thiophene-H), 7.43–7.39 (t, 2H, Ph-H; d, H, thiophene-H), 7.32 (t, H, Ph-H). <sup>13</sup>C NMR (400 MHz, DMSO-*d*<sub>6</sub>) δ 177.86(1C, C=S), 145.74(1C, C=N), 138.39(1C, thiophene-C), 137.76(1C, thiophene-C), 133.65(1C, Ph-C), 132.35(1C, Ph-C), 129.68(2C, Ph-C), 128.74(1C, thiophene-C), 125.88(2C, Ph-C), 124.84(1C, thiophene-C). MS (ESI): *m/z* 260.1 [M-H]<sup>-</sup>.

### 2.3. Determination of water solubility and lipid solubility

The experiment was performed as reference (Bai, Yan, Hu, Zhang, & Huang, 2006) described with minor modifications to determine the water/lipid solubility of selected compounds preliminarily. An excess of sample was dissolved in water/ethyl acetate, sonic disruption for 1 h, and oscillation incubation for 6 h in room temperature, after centrifugation for 10 min, the upper clear liquid was retained by filtration. 1 mL Filtrate was then diluted with water/ethyl acetate into five concentrations from saturated to low, then the absorbance values were recorded using a Shimadzu UV-2450 spectrophotometer (Japan) at its maximum absorption wavelength, and standard curve was determined. Known concentration of the sample solution(dissolved in water/ethyl acetate) was configured, recorded the absorbance value using a Shimadzu UV-2450 spectrophotometer (Japan) at its maximum absorption wavelength. Since dilute solution conformed to Lambert-Beer's law, according to the obtained standard curve and the absorbance value of known concentration, the sample's water solubility and lipid solubility can be calculated.

### 2.4. Tyrosinase activity assay

The assay of inhibition of target compounds on the diphenolase activity of mushroom tyrosinase was performed by our reported procedure with minor modifications (Xie et al., 2016). L-DOPA was used as substrate for the assay. The reaction media (3 mL) for activity assay contained 2.8 mL 0.5 mM L-DOPA in 50 mM Na<sub>2</sub>HPO<sub>4</sub>-NaH<sub>2</sub>PO<sub>4</sub> buffer (pH = 6.8) and 0.1 mL of different concentrations of inhibitor (dissolved by DMSO previously), and then 0.1 mL of the aqueous solution of mushroom tyrosinase(166.5 μg/mL) was added to the mixture. The solution was immediately monitored by measuring the linear increase in optical density at 475 nm of formation of the DOPA chrome for 150 s using a Shimadzu UV-2450 spectrophotometer (Japan). The extent of inhibition by the addition of the sample was expressed as the percentage necessary for 50% inhibition (IC<sub>50</sub>), calculated by SPSS19. The value of inhibition ratio of compounds on tyrosinase can be calculated by the following equation:

$$\text{Inhibition ratio (\%)} = (1 - \text{OD}_1/\text{OD}_2) \times 100\%$$

where OD<sub>1</sub> is the slope of reaction kinetics equation obtained from reaction with inhibitor; OD<sub>2</sub> is the slope of reaction kinetics

equation obtained from reaction with reagent blank. Kojic acid and thiophene dicarboxaldehyde thiosemicarbazone were used as reference standard inhibitors for comparison, respectively.

### 2.5. Determination of inhibition mechanism, inhibition type and inhibition constants

Determination of inhibition mechanism was assayed by maintaining the concentration of L-DOPA (0.5 mM) and changing the concentration of the enzyme (16, 12, 8, 4 μg/mL) in reaction medium. The enzyme activity was measured for different concentrations of inhibitor.

Determination of inhibition type and inhibition constants was assayed by maintaining the concentration of enzyme (10 μg/mL) and changing the concentration of the L-DOPA (0.5, 1, 1.5, 2 mM) in reaction medium. The inhibition type was assayed by the Lineweaver-Burk plot, the value of inhibition constants ( $K_i$ ,  $K_{IS}$ ) can be obtained by the following equation:  $\frac{1}{v} = \frac{K_m}{V_m[S]} \left(1 + \frac{[I]}{K_i}\right) + \frac{1}{V_m} \left(1 + \frac{[I]}{K_{IS}}\right)$  where  $v$  is the reaction velocity;  $K_m$  is the Michaelis constant;  $V_m$  is the maximal velocity;  $[I]$  is the concentration of inhibitor;  $[S]$  is the concentration of substrate;  $K_i$  is the constants for the inhibitor binding with the free enzyme and  $K_{IS}$  is the constants for the inhibitor binding with enzyme substrate complex, They were obtained from the slope or the vertical intercept versus the inhibitor concentration, respectively.

### 2.6. Fluorescence quenching titration

The experiment was performed as reference described with minor modifications (Wang, Zhang, Yan, & Gong, 2014). The reaction media (2 mL) contained 1.8 mL  $\text{Na}_2\text{HPO}_4\text{-NaH}_2\text{PO}_4$  buffer (pH = 6.8, 50 mM) and 0.2 mL of the aqueous solution of mushroom tyrosinase, and then titrated by successive addition of compounds **1**, **2**, **6** and **1-Cu<sup>2+</sup>** complex (the constituent ratio of ligand and  $\text{Cu}^{2+}$  was 2:1, the chelation ratio has been determined by continuous variation method) (Karikari, Mather, & Long, 2007) solution using a pipette (to final concentrations ranging from 0 to 105.6 μM). Fluorescence intensities were recorded using a Hitachi F-4600 spectrofluorophotometer (Japan) at three different temperatures (26, 31 and 36 °C) with an excitation wavelength of 280 nm, emission wavelength from 300 to 550 nm and excitation and emission slit widths of 5 nm.

Considering the inner-filter effect of fluorescence, all of the fluorescence intensities were corrected for the absorption of exciting light and reabsorption of emitted light in this study. The inner-filter effect can be corrected by the following formula (Bi, Yan, Wang, Pang, & Wang, 2012):

$$F_{\text{corr}} = F_{\text{obs}} e^{(A_1 + A_2)/2}$$

where  $F_{\text{cor}}$  and  $F_{\text{obs}}$  are the corrected and observed fluorescence intensities, respectively.  $A_1$  and  $A_2$  are the absorbances of inhibitor at the excitation and emission wavelengths, respectively.

Fluorescence quenching was described by the well-known Stern-Volmer equation:

$$\log \frac{F_0 - F}{F} = 1 + K_q \tau_0 [Q] = 1 + K_{SV} [Q]$$

where  $F_0$  and  $F$  are the fluorescence intensities before and after the addition of the quencher, respectively;  $K_q$  and  $K_{SV}$  are the bimolecular quenching constant and the Stern-Volmer quenching constant, respectively;  $\tau_0$  [ $10^{-8}$  s] (Xiao et al., 2007) is the average lifetime of the fluorophore in the absence of the quencher,  $[Q]$  is the concentration of the quencher.

For the static quenching interaction, if it is assumed that there are similar and independent sites in the biomolecule, the apparent

binding constant ( $K_a$ ) and the number of binding sites ( $n$ ) can be calculated by the following equation (Shahabadi, Maghsudi, & Rouhani, 2012):

$$\log \frac{F_0 - F}{F} = \log K_a + n \log [Q]$$

### 2.7. <sup>1</sup>H NMR and <sup>13</sup>C NMR titration

<sup>1</sup>H NMR titration studies were performed to investigate the interaction between the compounds **1**, **5**, **6** and tyrosinase, respectively. A 0.5 mL 28 mM solution of target compound in DMSO- $d_6$  was prepared and titrated with tyrosinase solution by using a micropipette (to final concentrations ranging from 1.42 to 2.84 mg/mL for compounds **1**, **5** and **6**). After each addition of tyrosinase, the <sup>1</sup>H NMR spectrum was recorded and the changes in the chemical shift of the protons were noted.

For further investigate the interaction between the compound **6** and tyrosinase, <sup>13</sup>C NMR titration studies were performed. The experiment was performed as <sup>1</sup>H NMR titration. A 0.5 mL 100 mM solution of compound **6** in DMSO- $d_6$  was prepared and titrated with tyrosinase solution by using a micropipette. After each addition of tyrosinase, the <sup>13</sup>C NMR spectrum was recorded.

### 2.8. IR and UV spectrum

In order to get further understanding manner and site of interaction between inhibitors and enzyme, complex (compound **6** and  $\text{Cu}^{2+}$ ) was synthesized (Bisceglie et al., 2014) and its IR and UV spectra were studied.

Compound **6** was dissolved in ethanol, and then copper sulfate solution (40 mM) was slowly added, finally lots of flocculent precipitate was generated. The turbid liquid was centrifuged, and precipitate was separated. The precipitate was washed with ethanol and water, and dried in a vacuum oven at 40 °C for 12 h. The IR spectra were measured with KBr pellets on a Nicolet 5700 FT-IR spectrometer in the range of 4000–400  $\text{cm}^{-1}$ . The UV-vis absorption spectrum were examined on a UV-2450 spectrophotometer (Japan) in the range 250 nm–500 nm using a 1.0 cm quartz cell at room temperature in the ethanol medium.

## 3. Results and discussion

### 3.1. Effects of thiophene 2-carboxaldehyde thiosemicarbazone derivatives on tyrosinase activities and the determination of water and lipid solubility

The values of  $\text{IC}_{50}$  of compounds **1–12** are listed in Table 1. Kojic acid and thiophene 2-carboxaldehyde thiosemicarbazone (TCT) were used as comparative reference standard inhibitors. As shown in Table 1, the inhibitory activity of compounds **1–12** were much stronger than that of Kojic acid; however, compared to TCT, only the inhibitory activity of compound **6** was better than that of its precursor. In our previous study, we found that the excellent tyrosinase inhibiting activity of the precursor was primarily based on the formation of complexes between the sulfur atom from the thiourea of the precursor and the copper ion of the enzyme center, with an auxiliary vicinity synergistic effect of the thiophene ring (Xie et al., 2016). From the experimental results, we found that the 4- and 5-functionalization of the thiophene ring of the precursor decreased the inhibitory activity of nearly every target modifier with only one exception. Thus, the increased steric hindrance by the 4- and 5-functionalization of the thiophene ring was crucial to inhibit the formation of complexes between the sulfur atom from the thiourea of the precursor and the copper ion of the enzyme center, and decreased the inhibition of the modifier,

**Table 1**  
Inhibitory activity of compounds **1–12** on tyrosinase in mushrooms; Water solubility and lipid solubility of precursor and compounds **1, 2, 3, 6**; The Stern-Volmer quenching constants  $K_{SV}$ , the quenching rate constants  $K_q$  and the binding constant  $K_b$ .

Compound	Precursor	1	2	3	4	5	6	7	8	9	10	11	12	Kojic acid
$R_1$	H	CH <sub>2</sub> OH	CH <sub>2</sub> OCH <sub>3</sub>	CH <sub>2</sub> OCH <sub>2</sub> -CH <sub>2</sub> OH	CH <sub>2</sub> OCH <sub>2</sub> -CH <sub>2</sub> OH	H	CH <sub>2</sub> OCO-CH <sub>3</sub>	H	CH <sub>2</sub> OCH <sub>3</sub>	H	CH <sub>2</sub> OCO-CH <sub>3</sub>	H	CH <sub>3</sub>	H
$R_2$	H	H	H	H	H	CH <sub>2</sub> OH	H	CH <sub>2</sub> OCH <sub>3</sub>	CH <sub>2</sub> OCH <sub>2</sub> -CH <sub>2</sub> OH	H	CH <sub>2</sub> OCO-CH <sub>3</sub>	CH <sub>3</sub>	NO <sub>2</sub>	Ph
IC <sub>50</sub> (μM)	0.43	0.67	0.74	0.49	1.42	3.21	0.34	1.77	3.26	1.71	1.71	2.59	3.53	0.67
Water-solubility (g/L)	0.138	0.335	0.147	0.402	-	-	0.262	-	-	-	-	-	-	-
Lipid-solubility (g/L)	9.386	6.063	2.817	15.890	-	-	17.722	-	-	-	-	-	-	-
$K_{SV}$ (10 <sup>4</sup> L·mol <sup>-1</sup> )	-	1.80	1.49	1.32	1.09	1.48	1.57	1.34	1.27	1.47	1.47	-	-	-
	-	31 °C	31 °C	31 °C	31 °C	31 °C	31 °C	31 °C	31 °C	31 °C	31 °C	-	-	-
$K_q$ (10 <sup>12</sup> L·mol <sup>-1</sup> ·s <sup>-1</sup> )	-	1.46	0.95	1.32	1.09	1.48	1.57	1.34	1.27	1.47	1.47	-	-	-
	-	36 °C	36 °C	36 °C	36 °C	36 °C	36 °C	36 °C	36 °C	36 °C	36 °C	-	-	-
$lgK_b$ (L·mol <sup>-1</sup> ·s <sup>-1</sup> )	-	5.19	4.61	4.83	4.54	4.38	5.07	4.59	4.02	4.22	4.22	-	-	-
	-	31 °C	31 °C	31 °C	31 °C	31 °C	31 °C	31 °C	31 °C	31 °C	31 °C	-	-	-
	-	3.83	4.03	4.03	4.03	4.03	4.03	4.03	4.03	4.03	4.03	-	-	-

especially for the 5-functionalization modifiers. Moreover, we found that 4-methoxyacetyl-thiophene-2-carbaldehyde thiosemicarbazone had a 20.93% decrease of IC<sub>50</sub> compared to that of its precursor (IC<sub>50</sub> = 0.43 μM), which was not explained successfully by its unfavourable effect of steric hindrance from introducing 4-substituted groups on thiophene ring of the TCT precursor. This may have occurred due to the presence of another force with a stronger effect that promoted the formation of these complexes and negated the inferior effect of steric hindrance. We assumed that this favorable effect came from the carbonyl oxygen atom of the methoxyacetyl group coordinating with the copper ion in the complexes, which was verified by results of NMR titration and IR spectra, and much stronger than the auxiliary vicinity synergistic effect of the thiophene ring on the precursor (Xie et al., 2016).

We also studied the inhibitory mechanism by compounds **1, 2, 5, 6, 7** and **9** against the tyrosinase for the oxidation of L-DOPA. The relationship between the enzymatic activity and the concentrations of the inhibitors was observed as groups of straight lines passing through the origin (Fig. S1), indicating that the inhibition was reversible. In addition, we investigated the inhibitory kinetics of tyrosinase in mushrooms using compounds **1, 2, 5, 6, 7** and **9**. The double-reciprocal plots yielded a group of straight lines intersecting at the second quadrant (Fig. S2), indicating that they were mixed-type inhibitors. The compounds were not only capable of binding with the free enzymes, but also with enzyme-substrate complexes.  $K_i$  and  $K_{iS}$  were obtained from the Lineweaver-Burk plot, as shown in Table S1. The values of  $K_{iS}$  were greater than the values of  $K_i$ , which indicated that the affinities of the compounds bonding with the free enzyme were greater than those of the compounds bonding with enzyme-substrate complexes.

Water solubility is a major factor in limiting drug absorption (O'Driscoll & Griffin, 2008). In drug design, predicting lipid solubility is important in identifying the proper excipients to solubilize and formulate drugs in lipid formulations (Rane & Anderson, 2008). Here, the water and lipid solubility of the parent compound and compounds **1, 2, 3** and **6** were preliminarily determined by UV Spectrophotometry. The values of the water and lipid solubility are listed in Table 1. Compared to the water solubility of the parent compound, the water solubility of compounds **1, 2, 3** and **6** improved slightly. The water solubility of all of compounds was less than 0.5 g/L, which indicated that the introduction of these groups, even the hydroxymethyl group, had a limited effect on improving water solubility. Compared to the lipid solubility of the parent compound, the lipid solubility of compounds **1** and **2** decreased significantly, while the lipid solubility of compounds **3** and **6** increased significantly, which showed that the extension of the hydrophobic chains improved lipid solubility.

### 3.2. Fluorescence studies

Studies in inhibition kinetics found that compounds tend to bond with free enzymes during catalysis, so that compounds form complexes with enzymes. We used fluorescence measurements to further investigate the interactions between compounds and tyrosinase. The fluorescence emission spectra of tyrosinase in the absence of and in the presence of compounds **1, 2** and **6** excited at 280 nm are shown in Fig. 2. Obviously, tyrosinase in an aqueous solution exhibited a strong fluorescence emission peak at 381 nm, and with the gradual addition of compounds **1, 2** and **6**, the fluorescence intensity of tyrosinase decreased remarkably without any significant peak changes, indicating that compounds **1, 2** and **6** interacted with tyrosinase and quenched its intrinsic fluorescence.

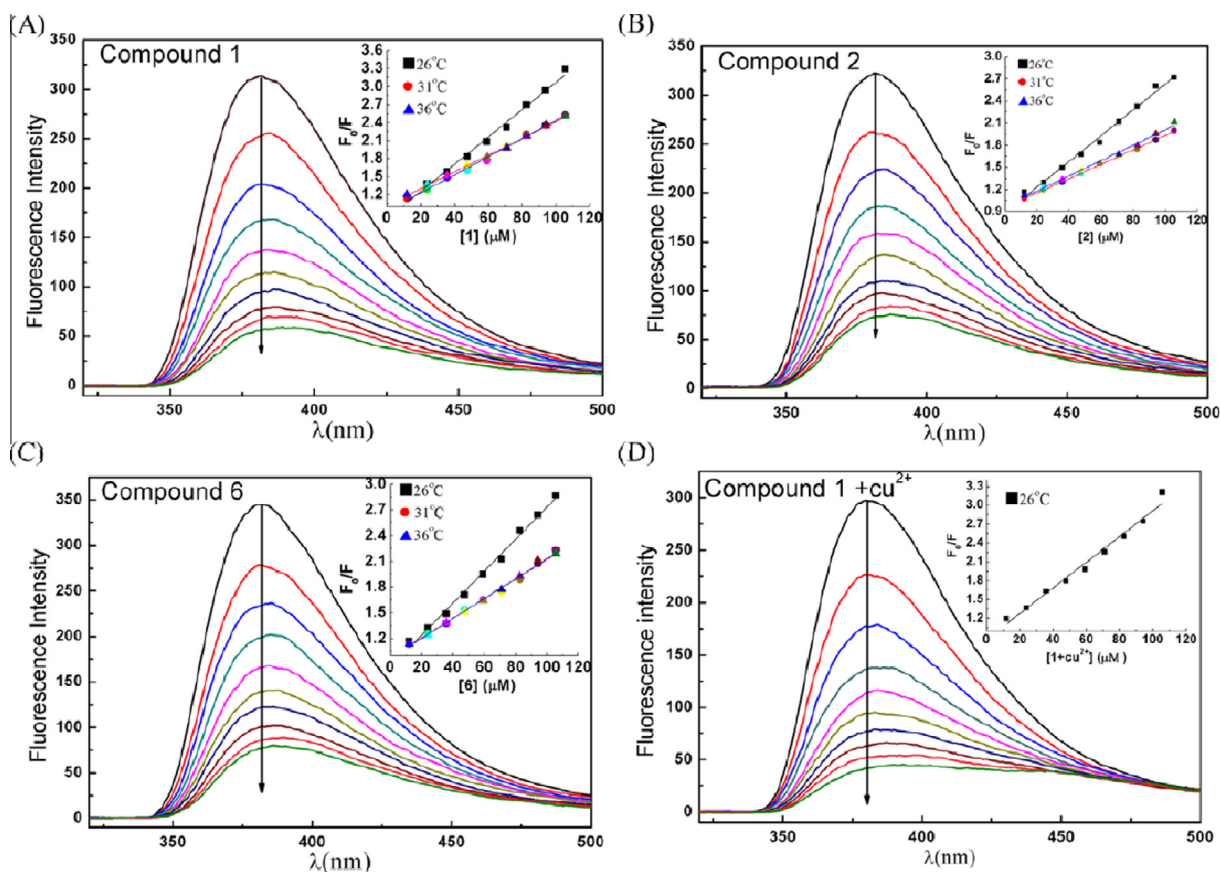


**Fig. 2.** Fluorescence spectra of tyrosinase in the presence of compounds **1**, **2**, **6** and the **1**-Cu<sup>2+</sup> complex at 26 °C. Concentrations for curves were 0, 12, 24, 36, 48, 59, 71, 83, 94 and 106 μM. The inset depicts Stern-Volmer plots for the fluorescence quenching of tyrosinase by compounds **1**, **2** and **6** at 26, 31 and 36 °C and the **1**-Cu<sup>2+</sup> complex at 26 °C.

The Stern-Volmer plots for the quenching of tyrosinase by compounds **1**, **2** and **6** (Fig. 2A–C) showed that they exhibited a linear relationship. The corresponding  $K_q$  values (Table 1) at different temperatures were much greater than the maximum scatter collision quenching constant of quenchers with biopolymers,  $2.0 \times 10^{10} \text{ L}\cdot\text{mol}^{-1}\cdot\text{s}^{-1}$  (Lakowicz, 2009), indicating that static quenching was dominant in the quenching process. Moreover, the  $K_a$  values (Table 1) appeared in a downward trend in the corresponding temperature-changed experiments, which further indicated that inhibitors quenched tyrosinase in a static process (Wang et al., 2014). When the quenching originated from complex formations between the quenchers and biopolymers, the forces involved in the interactions determined whether higher temperatures would increase or decrease the complex formation between the quenchers and biopolymers (Joye, Davidov-Pardo, Ludescher, & McClements, 2015). A significant decrease in the  $K_{SV}$  and  $K_a$  values occurred when the temperature rose from 26 to 31 °C, indicating that hydrogen bonding was dominant. This was expected due to the weakening of hydrogen bridges at high temperatures. When the temperature rose from 31 to 36 °C, the  $K_{SV}$  values appeared to be weakly temperature-dependent. The  $K_a$  value of compound **6** increased slightly only because the hydrogen bridges weakened at higher temperatures while the hydrophobic interactions increased, which led additional complex formations from the strengthening of the hydrophobic forces. (Joye et al., 2015). The results from the quenching of tyrosinase by compounds **1–9** and the values of  $IC_{50}$  of compounds **1–9** are listed in Table 1, and show that static quenching was dominant in the quenching process of compounds **3**, **4**, **5**, **7**, **8** and **9**, and that the  $K_a$  values of compounds **1–9** were almost inversely proportional to the values of  $IC_{50}$ .

To further investigate the acting site between the inhibitor and enzyme, we performed a fluorescence titration of tyrosinase with **1**-Cu<sup>2+</sup> complex. As illustrated in (Fig. 2D), the increased concentration of the **1**-Cu<sup>2+</sup> complex led to a greater decrease in the intensity of the emission band at 381 nm, unlike that of compound **1**. However, because of the overlap between the tyrosinase fluorescence and the **1**-Cu<sup>2+</sup> complex absorbance (Fig. S3), the decreased intensity was likely related to the quenching by the fluorescence resonance energy transfer (FRET) (Joye et al., 2015). The static quenching binding constant ( $K_a$ ) of the **1**-Cu<sup>2+</sup> complex was  $10^{4.61} \text{ L}\cdot\text{mol}^{-1}\cdot\text{s}^{-1}$  at 26 °C, less than the static quenching of the binding constant ( $K_a$ ) of **1** ( $10^{5.19} \text{ L}\cdot\text{mol}^{-1}\cdot\text{s}^{-1}$ ). The results showed that the copper ion may have occupied the inhibitor activity site after the coordination of the inhibitor and copper, which led decreased quenching of tyrosinase.

### 3.3. Bonding mode studies from <sup>1</sup>H NMR, <sup>13</sup>C NMR titration, IR and UV of synthesized complex of compound **6** and Cu<sup>2+</sup>

#### 3.3.1. Bonding mode studies from <sup>1</sup>H NMR and <sup>13</sup>C NMR titration

To investigate the bonding mode between the inhibitor and tyrosinase, we used <sup>1</sup>H NMR and <sup>13</sup>C NMR titrations to identify the bonding mode between different molecules by determining the chemical shifts of hydrogen and carbon atoms (Park, Sahoo, & Choi, 2016).

The interactions between compounds **1**, **5**, **6** and tyrosinase were observed from the <sup>1</sup>H NMR titrations in DMSO-*d*<sub>6</sub>. After each addition of tyrosinase to the inhibitor, the <sup>1</sup>H NMR plot was recorded (Fig. 3A). With the addition of 40 mg/mL of tyrosinase to the target compounds, the peaks at 11.37/11.36/11.40 ppm nearly disappeared (compounds **1**, **5** and **6**, of -NH-CS-, Hc for

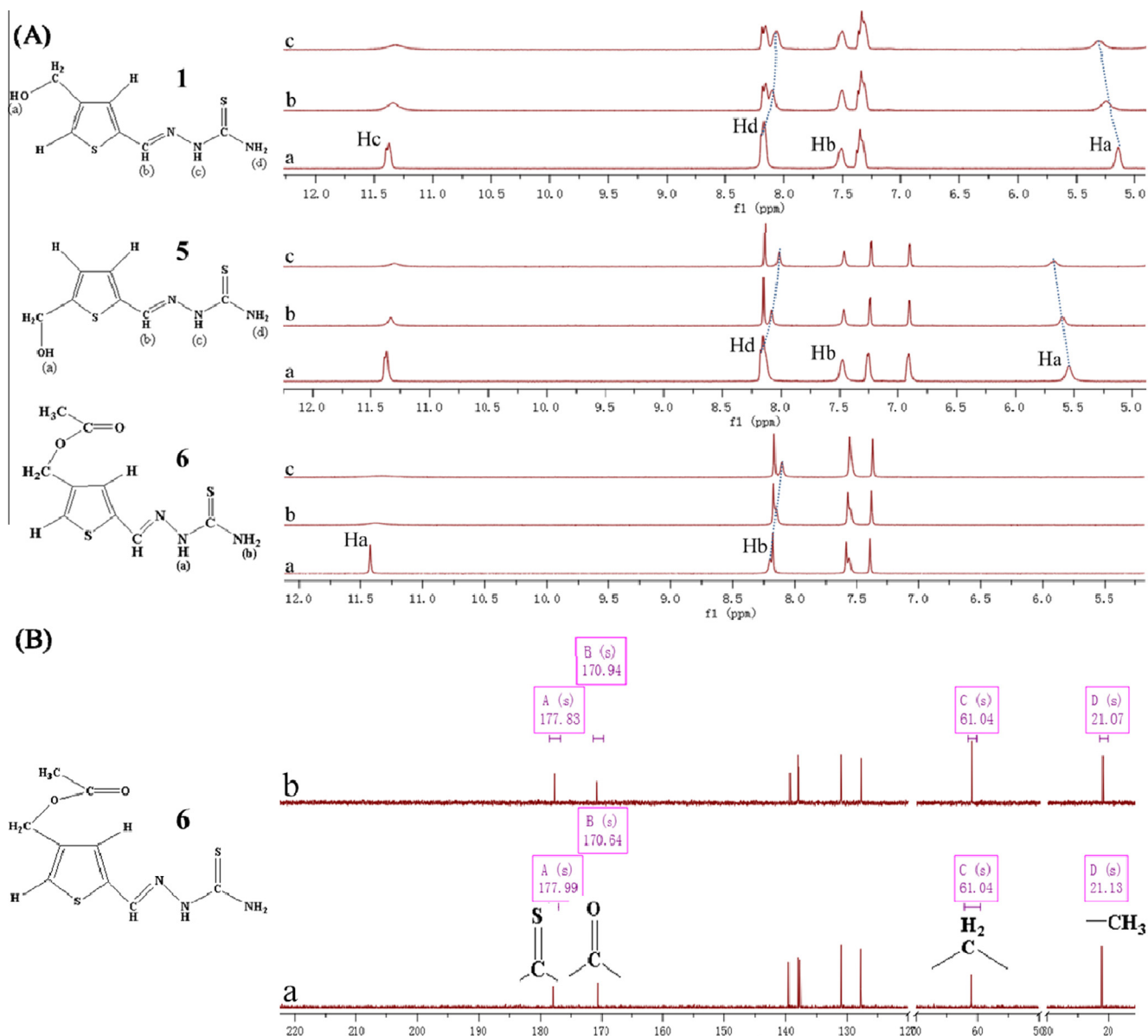


**Fig. 3.** (A)  $^1\text{H}$  NMR titration of compounds **1**, **5** and **6** (28 mM) with tyrosinase in the  $\text{DMSO-}d_6$  solvent. Concentrations of tyrosinase for curves a–c were 0, 1.42 and 2.84 mg/L. The lines in the figure represent the major changes in NMR spectrum; and (B)  $^{13}\text{C}$  NMR titration of compound **6** (100 mM) with tyrosinase in the  $\text{DMSO-}d_6$  solvent. Concentrations of tyrosinase for curves a–b were 0 and 5.56 mg/L.

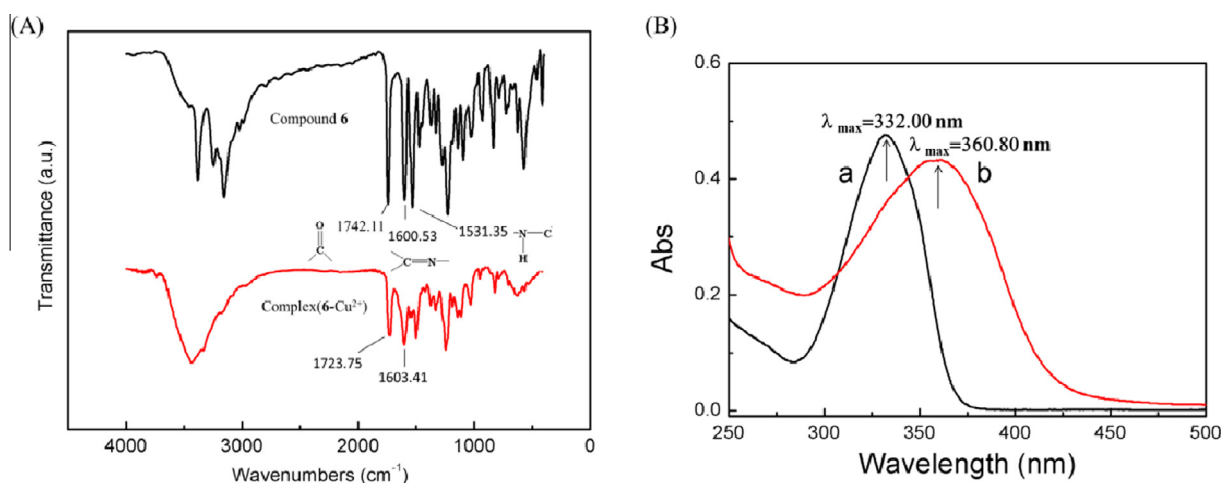


**Fig. 4.** (A) IR spectra of compound **6** and the complex  $(\mathbf{6-Cu}^{2+})$ ; and (B) UV spectra of compound **6**(a) and the complex  $(\mathbf{6-Cu}^{2+})$ (b).

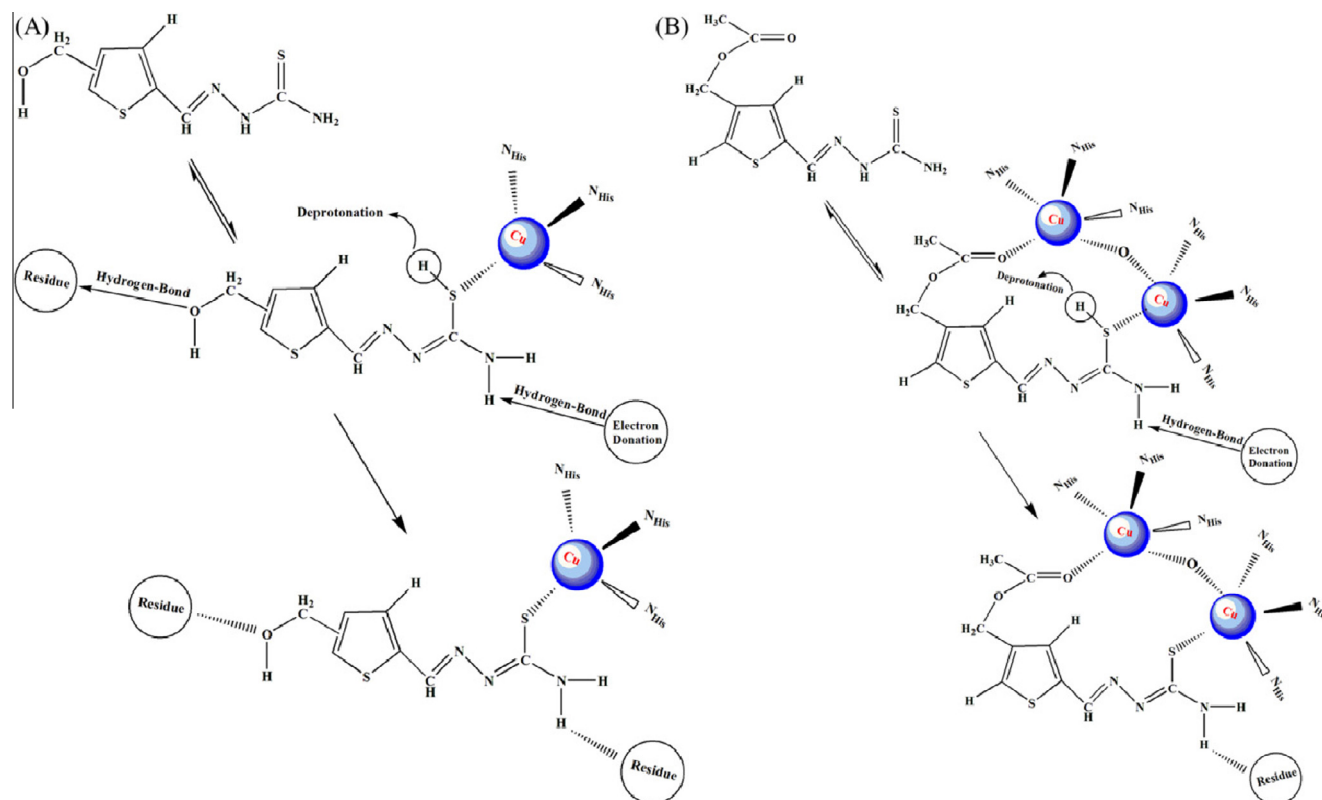


Fig. 5. (A) Plausible binding mode of compounds **1** and **5** with tyrosinase; and (B) plausible binding mode of compound **6** with tyrosinase.

compounds **1** and **5**, Ha for compound **6**). This was caused by the tautomeric effect, in which  $\text{NH}-\text{C}=\text{S}$  was transformed into  $\text{N}=\text{C}-\text{SH}$ . Then, the sulfur atom donated hydrogen and formed a complex with enzymic  $\text{Cu}^{2+}$  and led to the disappearance of the  $-\text{CSNH}-$  proton. With the addition of tyrosinase to the target compound **1** or **5** or **6**, the peaks at 8.17/8.13/8.16 ppm (amino proton,  $-\text{NH}_2$ , Hd for compounds **1** and **5**, Hb for compound **6**) split, and the chemical shifts of one proton moved upfield (8.06/8.01/8.09 ppm), which indicated that the increased electron density on the amino proton resulted from the formation of the hydrogen bond between hydrogen atom of the  $-\text{NH}_2$  group and tyrosinase.

Meanwhile, the peaks at 5.13/5.53 ppm for compounds **1** and **5** (Ha,  $\text{CH}_2-\text{OH}$ ) gradually shifted downfield (5.32/5.67 ppm), which indicated that the decrease of the electron density on the hydroxyl proton resulted from the formation of the hydrogen bond between the oxygen atom of the  $-\text{OH}$  group and the amino residue of tyrosinase.

The interactions between compound **6** and tyrosinase were further observed from the  $^{13}\text{C}$  NMR titrations in  $\text{DMSO}-d_6$  (Fig. 3B). Upon the addition of 60 mg/mL of tyrosinase to compound **6**, the peaks at 177.99 ppm moved upfield (177.83 ppm), which indicated that the electron density increased in the carbon atom on the thiocarbonyl group. This occurred because the conjugated effect increased the electron density in the carbon atom after the formation of the complex. The peaks at 170.64 ppm moved downfield (170.94 ppm), which indicated that the electron density decreased in the carbon atom on the carbonyl group. This may be explained because the oxygen atom of the carbonyl group formed a coordination bond with the copper ions ( $\text{C}=\text{O} \rightarrow \text{Cu}^{2+}$ ) of the enzyme, which caused the electron density of the oxygen atoms to decrease and electronegativity to increase. Thus, the electron density of the adjacent carbon atom on the carbonyl group decreased by enhancing the  $\sigma$ -effect of the carbonyl oxygen. From these results, we

assumed that compound **6** combined with the enzyme by forming a complex between the thiocarbonyl/carbonyl group and the dinuclear copper ions in the active center of tyrosinase, which differed from the interaction mode of compounds **1** and **5**. This assumption was reinforced by the experimental data of IR and UV spectrum studies of the synthesized complex of the compound **6** and  $\text{Cu}^{2+}$ , which was a mimic complex between compound **6** and enzyme.

### 3.3.2. Bonding mode studies from $^1\text{H}$ NMR, $^{13}\text{C}$ NMR titration of inhibitors and enzymes, and the IR and UV of the synthesized complex of compound **6** and $\text{Cu}^{2+}$

To further verify the above assumption of the bonding mode between compound **6** and the enzyme, a mimic complex of the inhibitor and enzyme was synthesized and then the IR and UV spectra were determined. As shown in (Fig. 4B), the UV spectra displayed a redshift, which indicated that the formation of the complex led to a d-d electronic transition. Further, by comparing the IR spectra (Fig. 4A) of compound **6** and the complex of compound **6** and  $\text{Cu}^{2+}$ , we found that the intrinsic carbonyl stretch vibration changed from  $1742.11\text{ cm}^{-1}$  to  $1723.75\text{ cm}^{-1}$ , which was introduced by the formation of complex bonding between the carbonyl oxygen of compound **6** and  $\text{Cu}^{2+}$ , and led to a weaker double bond in the carbonyl group (Li et al., 2014). Moreover, the stretching vibration of the carbon-nitrogen double bond was practically unchanged (from  $1600.53\text{ cm}^{-1}$  to  $1603.41\text{ cm}^{-1}$ ). Amide II peaks ( $1535.15\text{ cm}^{-1}$ ) (Guo, Kimura, & Furutani, 2013) nearly disappeared, which suggested that when the thiocarbonyl group formed a coordinating bond with the copper ions, the resulting conjugate structure ( $\text{N}=\text{C}-\text{SH}$ ) led to disappearance of the  $-\text{CSNH}-$  proton by tautomerization (Xie et al., 2016). The above results and IR spectra were consistent with the results of the  $^1\text{H}$  NMR/ $^{13}\text{C}$  NMR titrations.

Based on these results, we proposed a plausible binding mode of compounds **1**, **5** and **6** with tyrosinase in Fig. 5.

#### 4. Conclusion

We synthesized a series of 4-functionalized and 5-functionalized thiophene-2-carbaldehyde thiosemicarbazone derivatives (**1–12**), and investigated their water and lipid solubility, inhibitory activities and mechanisms on tyrosinase in mushrooms using Spectrofluorimetry,  $^1\text{H}$  and  $^{13}\text{C}$  NMR titration and IR spectra. We found that the strong auxiliary vicinity synergistic effect from the 4-methoxyacetyl substitution group of 4-Methoxyacetyl-thiophene-2-carbaldehyde thiosemicarbazone promoted the inhibitory activity of the derivatives by promoting the formation complexes between the sulfur atom of the thiourea group in the inhibitor and the dicopper ions of the enzyme active center. The effects of the hydrophobic and hydrogen bonds were also determined. The 4-methoxyacetyl substitution of the thiophene-2-carbaldehyde thiosemicarbazone successfully produced novel inhibitors of tyrosinase in mushroom. Additional research is necessary to develop novel and highly potent tyrosinase inhibitors.

#### Acknowledgments

This work was supported by National Natural Sciences Foundation of China (No. 20962014) and the free searching foundation of State Key Laboratory of Food Science and Technology (Nanchang University) in China (SKLF-TS-200914).

#### Appendix A. Supplementary data

Supplementary data associated with this article can be found, in the online version, at <http://dx.doi.org/10.1016/j.foodchem.2016.10.140>.

#### References

- Arung, E. T., Kusuma, I. W., Iskander, Y. M., Yasutake, S., Shimizu, K., & Kondo, R. (2005). Screening of Indonesian plants for tyrosinase inhibitory activity. *Journal of Wood Science*, *51*, 520–525.
- Bisceglie, F., Pinelli, S., Alinovi, R., Goldoni, M., Mutti, A., & Camerini, A. (2014). Cinnamaldehyde and cuminaldehyde thiosemicarbazones and their copper(II) and nickel(II) complexes: A study to understand their biological activity. *Journal of Inorganic Biochemistry*, *140*, 111–125.
- Bai, T. C., Yan, G. B., Hu, J., Zhang, H. L., & Huang, C. G. (2006). Solubility of silybin in aqueous poly(ethylene glycol) solution. *International Journal of Pharmaceutics*, *308*, 100–106.
- Bi, S. Y., Yan, L. L., Wang, Y., Pang, B., & Wang, T. J. (2012). Spectroscopic study on the interaction of eugenol with salmon sperm DNA in vitro. *Journal of Luminescence*, *132*, 2355–2360.
- CDER, & FDA. (1996). Guidance for industry: single dose acute toxicity testing for pharmaceuticals (Final).
- Chang, T. S. (2009). An updated review of tyrosinase inhibitors. *International Journal of Molecular Sciences*, *10*, 2440–2475.
- Choi, J., Park, S. J., & Jee, J. G. (2015). Analogues of ethionamide, a drug used for multidrug-resistant tuberculosis, exhibit potent inhibition of tyrosinase. *European Journal of Medicinal Chemistry*, *106*, 157–166.
- Chen, B. N., Xing, R., Wang, F., Zheng, A. P., & Wang, L. (2015). Inhibitory effects of  $-\text{Na}_8\text{SiW}_{11}\text{CoO}_{40}$  on tyrosinase and its application in controlling browning of fresh-cut apples. *Food Chemistry*, *188*, 177–183.
- Cordier A. (1991). Single dose toxicity: Industry perspectives. In: P. F. D'Arcy, & D. W. G. Harron (Eds.), *Proceedings of the first international conference on harmonization* (pp. 189–191). Brussels.
- Guo, H., Kimura, T., & Furutani, Y. (2013). Distortion of the amide-I and -II bands of an  $\alpha$ -helical membrane protein, pharaonis halorhodopsin, depends on thickness of gold films utilized for surface-enhanced infrared absorption spectroscopy. *Chemical Physics*, *419*, 8–16.
- Guo, Z. R., Yang, G. Z., Chu, F. M., Xu, G. S., Zhang, J. J., Zhang, S. R., & Yu, Y. W. (1989). Studies on antipeptic ulcer agents: The synthesis and structure-activity relationship analysis of heterocycle aldehyde (Thio) semicarbazones and acyl hydrazones. *Chinese Acta Pharmaceutica Sinica*, *24*(10), 737–743.
- Joye, I. J., Davidov-Pardo, G., Ludescher, R. D., & McClements, D. J. (2015). Fluorescence quenching study of resveratrol binding to zein and gliadin: Towards a more rational approach to resveratrol encapsulation using water-insoluble proteins. *Food Chemistry*, *185*, 261–267.
- Karikari, A. S., Mather, B. D., & Long, T. E. (2007). Association of star-shaped poly(D,L-lactide)s containing nucleobase multiple hydrogen bonding. *Biomacromolecules*, *8*, 302–308.
- Li, L. J., Fu, J., Qiao, Y., Wang, C., Huang, Y. Y., Liu, C. C., et al. (2014). Synthesis, characterization and cytotoxicity studies of platinum(II) complexes with reduced amino acid ester Schiff-bases as ligands. *Inorganica Chimica Acta*, *419*, 135–140.
- Lakowicz, J. R. (2009). *Principles of fluorescence spectroscopy*. New York: Springer Publications.
- Motabo, Y., Kumagai, T., Yamamoto, A., Yoshitsu, H., & Sugiyama, M. (2006). Crystallographic evidence that the dinuclear copper center of tyrosinase is flexible during catalysis. *Journal of Biological Chemistry*, *281*, 8981–8990.
- Mendes, E., Perry, M. d. J., & Francisco, A. P. (2014). Design and discovery of mushroom tyrosinase inhibitors and their therapeutic applications. *Expert Opinion on Drug Discovery*, *9*, 533–554.
- O'Driscoll, C. M., & Griffin, B. T. (2008). Biopharmaceutical challenges associated with drugs with low aqueous solubility—The potential impact of lipid-based formulations. *Advanced Drug Delivery Reviews*, *60*, 617–624.
- Park, J. O., Sahoo, K. S., & Choi, H. J. (2016). Design, synthesis and  $^1\text{H}$  NMR study of C $_{3v}$ -symmetric anion receptors with urethane-NH as recognition group. *Spectrochimica Acta Part A: Molecular and Biomolecular Spectroscopy*, *153*, 199–205.
- Pan, T., Li, X., & Jankovic, J. (2011). The association between Parkinson's disease and melanoma. *International Journal of Cancer*, *128*, 2251–2260.
- Rane, S. S., & Anderson, B. D. (2008). What determines drug solubility in lipid vehicles: Is it predictable? *Advanced Drug Delivery Reviews*, *60*, 638–656.
- Shi, Y., Chen, Q. X., Wang, Q., Song, K. K., & Qiu, L. (2005). Inhibitory effects of cinnamic acid and its derivatives on the diphenolase activity of mushroom (*Agaricus bisporus*) tyrosinase. *Food Chemistry*, *92*, 707–712.
- Sabadak, T., Demirkiran, O., Ozturk, M., & Topcu, G. (2013). Phenolic compounds from *Trifolium echinatum* Bieb. and investigation of their tyrosinase inhibitory and antioxidant activities. *Phytochemistry*, *96*, 305–311.
- Song, K. K., Huang, H., Han, P., Zhang, C. L., Shi, Y., & Chen, Q. X. (2006). Inhibitory effects of cis- and trans-isomers of 3,5-dihydroxystilbene on the activity of mushroom tyrosinase. *Biochemical and Biophysical Research Communications*, *342*, 1147–1151.
- Shahabadi, N., Maghsudi, M., & Rouhani, S. (2012). Study on the interaction of food colourant quinoline yellow with bovine serum albumin by spectroscopic techniques. *Food Chemistry*, *135*, 1836–1841.
- Seo, S. Y., Sharma, V. K., & Sharma, N. (2003). Mushroom tyrosinase: Recent prospects. *Journal of Agricultural and Food Chemistry*, *51*, 2837–2853.
- Wang, Y. J., Zhang, G. W., Yan, J. K., & Gong, D. M. (2014). Inhibitory effect of morin on tyrosinase: Insights from spectroscopic and molecular docking studies. *Food Chemistry*, *163*, 226–233.
- Xiao, J. B., Chen, J. W., Cao, H., Ren, F. L., Yang, C. S., Chen, Y., et al. (2007). Study of the interaction between baicalin and bovine serum albumin by multi-spectroscopic method. *Journal of Photochemistry and Photobiology A: Chemistry*, *191*, 222–227.
- Xie, J., Dong, H. H., Yu, Y. Y., & Cao, S. W. (2016). Inhibitory effect of synthetic aromatic heterocycle thiosemicarbazone derivatives on mushroom tyrosinase: Insights from fluorescence,  $^1\text{H}$  NMR titration and molecular docking studies. *Food Chemistry*, *190*, 709–716.
- Yin, S. J., Liu, K. J., Lee, J., Yang, J. M., Qian, G. Y., Si, Y. X., et al. (2015). Effect of hydroxysafflower yellow A on tyrosinase: Integration of inhibition kinetics with computational simulation. *Process Biochemistry*, *50*, 2112–2120.
- Zhu, Y. J., Song, K. K., Li, Z. C., Pan, Z. Z., Guo, Y. J., Zhou, J. J., et al. (2009). Antityrosinase and antimicrobial activities of trans-cinnamaldehyde thiosemicarbazone. *Journal of Agricultural and Food Chemistry*, *57*, 5518–5523.